contribution is the largest one. It decreases when the two unpaired electrons delocalize in wide or different regions of space. For "similar" bridges, the substitution of sulfur and nitrogen to oxygen shows that the less electronegative character of an atom and/or the more diffuse character of its AO's enhance the delocalization. The leading antiferromagnetic term is the kinetic exchange, which is greater the smaller the monocentric Coulomb integral is, that is the more important the delocalization is. Consequently, the large spatial extent of the magnetic orbitals favors the antiferromagnetic coupling.

Registry No. A, 83928-08-9.

Contribution from the Laboratoire de Spectrochimie des Elêments de Transition, ERA 672, Université de Paris-Sud, 91405 Orsay, France, Laboratoire de Chimie de Coordination du CNRS, Associé à l'Université Paul Sabatier, 31400 Toulouse, France, and Laboratoire de Chimie Structurale des Matériaux, Université Pierre et Marie Curie, 75232 Paris, France

Design of μ-Oxalato Copper(II) Binuclear Complexes Exhibiting Expected Magnetic Properties

MIGUEL JULVE,[1a] MICHEL VERDAGUER,[1a] ALAIN GLEIZES,[1b] MICHÈLE PHILOCHE-LEVISALLES,[1c] and OLIVIER KAHN*[1a]

Received April 9, 1984

The goal of this paper is to extract some basic concepts from the theory of the interaction between magnetic metal centers in coupled polymetallic systems and to show how they can be used to design μ-oxalato copper(II) binuclear complexes in which the magnitude of the antiferromagnetic coupling can be *tuned*. The two main concepts are those of *magnetic orbital*, defined as the singly occupied molecular orbital in a monomeric fragment, and of *overlap* between two magnetic orbitals in the binuclear unit. The magnitude of the antiferromagnetic interaction is expected to vary as the square of this overlap. In a $[LCu(C_2O_4)CuL']^{2+}$ binuclear cation, where L and L' are terminal ligands, the two monomeric fragments $LCu(C_2O_4)$ and $L'Cu(C_2O_4)$ do actually exist. According to the nature of L and L', the spatial orientation of the magnetic orbitals may be predicted, as well as the overlap between them. To test this approach, the synthesis, the crystal structures, and the magnetic properties of three new complexes are described: $[tmen(H_2O)Cu(C_2O_4)Cu(H_2O)tmen](ClO_4)_2 \cdot 1.25H_2O$ (**1**), $[dienCu(C_2O_4)Cu(H_2O)_2tmen](ClO_4)_2$ (**2**), and $[tmen(2\text{-MeIm})Cu(C_2O_4)Cu(2\text{-MeIm})tmen](PF_6)_2$ (**3**), where tmen = *N,N,N',N'*-tetramethylethylenediamine, dien = diethylenetriamine, and 2-MeIm = 2-methylimidazole. **1** crystallizes in the triclinic system, space group $P\bar{1}$ (a = 18.955 (3), b = 10.019 (3), c = 7.658 (3) Å; α = 98.30 (3), β = 98.37 (3), γ = 88.19 (2)°; Z = 2). Each copper atom is in a square-pyramidal environment with the two nitrogen atoms of tmen and two oxygen atoms of $C_2O_4^{2-}$ in the basal plane and a water molecule occupying the apical position. **2** crystallizes in the monoclinic system, space group $P2_1/c$ (a = 11.821 (4), b = 9.093 (3), c = 23.998 (6) Å; β = 96.50 (4)°; Z = 4). On the dien side, the four nearest neighbors of copper are the three nitrogen atoms of dien and only one oxygen atom of $C_2O_4^{2-}$; on the tmen side, the basal plane is again made of two oxygen atoms of $C_2O_4^{2-}$ and two nitrogen atoms of tmen. **3** crystallizes in the triclinic system, space group $P\bar{1}$ (a = 8.224 (2), b = 10.414 (3), c = 11.754 (3) Å; α = 94.63 (2), β = 108.57 (2), γ = 103.1 (2)°; Z = 2). The environment of each copper is intermediate between the square pyramid with only one oxygen atom of $C_2O_4^{2-}$ in the basal plane and the trigonal bipyramid. The magnetic properties of the three compounds were investigated in the 2-300 K temperature range and the singlet-triplet energy gaps deduced from the magnetic data were found as -385.4 cm^{-1} for **1**, -75.5 cm^{-1} for **2**, and -13.8 cm^{-1} for **3**. These values are compared to our previsions. Finally, the perspectives and the limits of such a molecular engineering of the coupled systems are discussed.

Introduction

The problem of the electronic structure of the coupled polymetallic systems has attracted the attention of a very large number of researchers. The main reason is probably that the phenomenon of interaction between metal centers lies at the meeting point of two apparently widely separated areas, namely the physics of the magnetic materials and the role of the polymetallic sites in the biological processes. Several orbital models have been proposed to describe the phenomenon of exchange interaction, and the controversies on the respective advantages and limits of each of them are still active.[2,3]

One of the goals of our group is to extract some basic ideas from these models and to show how they can be used to predict the nature of the transition ions and of the terminal and bridging ligands that must be utilized and the geometry that has to be achieved to obtain an interaction between the metal ions agreeing in sign and magnitude with the predicted values. In other words, we are attempting to lay the foundation of a molecular engineering of the coupled systems.[4]

In the last few years, several structural-magnetic correlations have been proposed.[5-11] In general, a dependence of the isotropic exchange parameter on some structural factors such as a bridging or a twist angle has been demonstrated. These correlations represent quite an important step in understanding the mechanism of the interaction. They cannot, however, be considered to be actual contributions to this molecular engineering. Indeed, except in very few cases, it seems extremely difficult to control the value of these structural parameters during the synthetic process. For instance, in dibridged copper(II) dimers like

(1) (a) Université de Paris-Sud. (b) Université Paul Sabatier. (c) Université Pierre et Marie Curie.
(2) Gatteschi, D., Kahn, O., Willett, R. D., Eds. *NATO Adv. Study Inst. Ser., Ser. C*, in press.
(3) Van Kalkeren, G.; Schmidt, W. W.; Block, R. *Physica B+C (Amsterdam)* **1979**, *97B+C*, 315-337.
(4) Kahn, O. *Inorg. Chim. Acta* **1982**, *62*, 3-14.
(5) Crawford, W. H.; Richardson, H. W.; Wasson, J. R.; Hodgson, D. J.; Hatfield, W. E. *Inorg. Chem.* **1976**, *15*, 2107-2110.
(6) Landee, C. P.; Willett, R. D. *Inorg. Chem.* **1981**, *20*, 2521-2525.
(7) Scaringe, R. P.; Hodgson, D. J.; Hatfield, W. E. *Transition Met. Chem. (Weinheim, Ger.)* **1981**, *6*, 340-344.
(8) Livermore, J. C.; Willett, R. D.; Gaura, R. M.; Landee, C. P. *Inorg. Chem.* **1982**, *21*, 1403-1405.
(9) Marsh, W. E.; Hatfield, W. E.; Hodgson, D. J. *Inorg. Chem.* **1982**, *21*, 2679-2684.
(10) Fletcher, R.; Hansen, J. J.; Livermore, J.; Willett, R. D. *Inorg. Chem.* **1983**, *22*, 330-334.
(11) Glerup, J.; Hodgson, D. J.; Pedersen, E. *Acta Chem. Scand., Ser. A* **1983**, *A37*, 161-164.

0020-1669/84/1323-3808$01.50/0

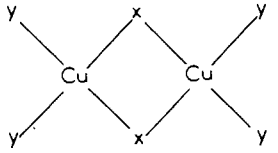

the value of the CuXCu bridging angles, which has been shown to play the key role in the sign and the magnitude of the singlet–triplet (S–T) energy gap, depends in an almost unforeseeable fashion on the nature of the terminal ligands or of the counteranions.[5]

In this paper, it will be shown that in the case of the μ-oxalato copper(II) binuclear complexes, the S–T energy gap can be controlled by the nature of the terminal ligands bound to the copper(II) ions.

The next section will briefly recall some basic concepts allowing the design of polymetallic systems exhibiting specific magnetic properties. Then we shall show how these concepts can be applied to the case of the μ-oxalato copper(II) complexes and can lead to predictions of the magnitude of the interaction in these complexes. In order to check whether these predictions are valid, we shall describe the synthesis, the crystal structure, and the magnetic properties of three new μ-oxalato copper(II) complexes, namely $[tmen(H_2O)Cu(C_2O_4)Cu(H_2O)tmen](ClO_4)_2 \cdot 1.25H_2O$ (**1**), where tmen = *N,N,N',N'*-tetramethylethylenediamine, $[dienCu(C_2O_4)Cu(H_2O)_2tmen](ClO_4)_2$ (**2**), where dien = diethylenetriamine, and $[tmen(2\text{-MeIm})Cu(C_2O_4)Cu(2\text{-MeIm})tmen](PF_6)_2$ (**3**), where 2-MeIm = 2-methylimidazole. Finally, we shall discuss the perspectives of this molecular engineering and the difficulties that remain to be overcome. A preliminary communication on this work was recently published.[12]

Basic Concepts[2,3,13-16]

Let us consider an A–B binuclear copper(II) complex in which A (or B) symbolizes one of the metal ions surrounded by its bridging and terminal ligands. In many systems, the A and B monomeric fragments are somewhat arbitrarily defined. In some cases, such as the μ-oxalato copper(II) complexes, these monomeric fragments do, however, exist, as will be shown hereafter. The unpaired electrons in A and B occupy the magnetic orbitals ϕ_A and ϕ_B, respectively, which can be defined as the highest singly occupied molecular orbitals in the A and B fragments. From the ground configuration $\phi_A\phi_B$ two low-lying states arise: a spin singlet and a spin triplet separated by J. The appropriate orbital parts of the wave functions are $|2(1 \pm S^2)|^{-1/2}|\phi_A(1)\,\phi_B(2) \pm \phi_A(2)\,\phi_B(1)|$, where + holds for the singlet and − for the triplet. S is the overlap integral:

$$S = \langle \phi_A(1) | \phi_B(1) \rangle \tag{1}$$

If we define the Hamiltonian of the problem as

$$\mathcal{H} = h(1) + h(2) + 1/r_{12} \tag{2}$$

where only the two magnetic electrons are considered as active, J can be expanded up to the first order in S according to

$$J = 4tS + 2j \tag{3}$$

with

$$t = \left\langle \phi_A(1) \left| h(1) - \frac{\alpha_A + \alpha_B}{2} \right| \phi_B(1) \right\rangle$$
$$\alpha_A = \langle \phi_A(1) | h(1) | \phi_A(1) \rangle \tag{4}$$
$$j = \langle \phi_A(1)\,\phi_B(2) | r_{12}^{-1} | \phi_A(2)\,\phi_B(1) \rangle$$

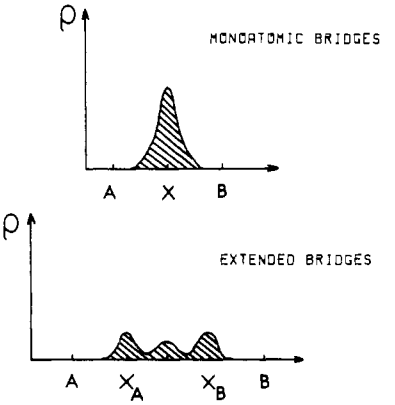

Figure 1. Schematic representations of overlap density in the cases of monoatomic bridges (top) and extended bridges (bottom).

Within the same level of approximation, J may also be expressed as

$$J = -2S(\Delta^2 - \delta^2)^{1/2} + 2j \tag{5}$$

where Δ is the energy gap between the two singly occupied MO's in A–B for the triplet state and δ the energy gap between the two magnetic orbitals ϕ_A and ϕ_B. The first term on the right-hand side of (3) and (5) is negative or zero and represents the antiferromagnetic contribution J_{AF} and the second term, $2j$, which is always positive, represents the ferromagnetic contribution J_F. It is usual to assume that t in (3) is proportional to S. Therefore, J_{AF} appears as proportional to S^2. The magnitude of $J_F = 2j$ according to the relative orientations of the magnetic orbitals in networks like **4** was discussed in

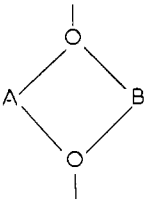

4

detail in two previous papers.[17,18] It was emphasized that this magnitude was governed by the extrema of the overlap density $\rho(i)$ between the magnetic orbitals defined as

$$\rho(i) = \phi_A(i)\,\phi_B(i) \tag{6}$$

In **4**, these extrema, positive or negative, may be very pronounced and J_F may be large. In contrast, in binuclear complexes with extended bridging ligands like oxalato, each magnetic orbital is delocalized over a large number of bridging atoms, so that the overlap density $\rho(i)$ is diffuse over the whole bridge without any peak of strong magnitude. This difference between binuclear complexes with monoatomic bridges and binuclear complexes with extended bridges as for the overlap density is schematized in Figure 1. In this latter case, the overlap integral

$$S = \int_{space} \rho(i)\, d\tau_i$$

may be large, but the self-repulsion of the overlap density

$$j = \int_{space} \frac{\rho(i)\,\rho(j)}{r_{ij}}\, d\tau_i\, d\tau_j$$

(12) Julve, M.; Verdaguer, M.; Kahn, O.; Gleizes, A.; Philoche-Levisalles, M. *Inorg. Chem.* **1983**, *22*, 368–370.
(13) Kahn, O.; Briat, B. *J. Chem. Soc., Faraday Trans. 2* **1976**, *72*, 268–281.
(14) Girerd, J. J.; Charlot, M. F.; Kahn, O. *Mol. Phys.* **1977**, *34*, 1063–1076.
(15) Kahn, O.; Charlot, M. F. *Nouv. J. Chim.* **1980**, *4*, 567–576.
(16) Charlot, M. F.; Kahn, O.; Drillon, M. *Chem. Phys.* **1982**, *70*, 177–187.
(17) Kahn, O.; Galy, J.; Journaux, Y.; Jaud, J.; Morgenstern-Badarau, I. *J. Am. Chem. Soc.* **1982**, *104*, 2165–2176.
(18) Journaux, Y.; Kahn, O.; Zarembowitch, J.; Galy, J.; Jaud, J. *J. Am. Chem. Soc.* **1983**, *105*, 7585–7591.

will remain weak. In other words, it can be expected that the ferromagnetic contribution J_F calculated from the nonorthogonal magnetic orbitals defined above is weak when the metal centers are bridged by polyatomic extended ligands.[19] This point will be discussed again in the last section. We assume that this is the case for the μ-oxalato complexes. It follows that, in these systems, the magnitude of J is essentially governed by S^2, the square of the overlap integral between the magnetic orbitals.

Magnetic Orbitals in μ-Oxalato Copper(II) Complexes

Owing to the Jahn–Teller plasticity of the coordination sphere around the copper(II),[20] this ion often adopts a coordination 4, or 4 + 1, or 4 + 2 with four nearest neighbors in the basal plane and eventually one or two next nearest neighbors in apical position. The unpaired electron is then described by a d_{xy}-type orbital pointing from the metal toward the nearest neighbors in an antibonding fashion as shown in **5**. When the symmetry of the chromophore is lower than C_s,

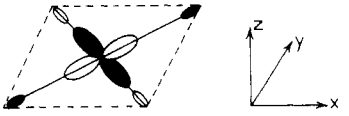

5

the unpaired electron is described by a $(d_{xy} + \lambda d_{z^2})$-type orbital, with some spin density on the apical sites. In the 4 + 1 coordination, the copper(II) can also acquire some trigonal-bipyramidal character, which again gives a nonzero spin density on the farthest ligand (see below). When there is a competition between oxygen and nitrogen atoms as nearest neighbors, the copper(II) most often first chooses the nitrogen atoms and then eventually completes its basal plane with oxygen atoms.

In the mononuclear complex $tmenCu(C_2O_4)\cdot 4H_2O$, the four nearest neighbors are the two nitrogen atoms (N_1 and N_2) of tmen and two oxygen atoms (O_1 and O_2) of the oxalate, a water molecule occupying the apical position.[21] The unpaired electron is then described by the orbital

$$\varphi = N\{d_{xy} - \alpha[\sigma(O_1) + \sigma(O_2)] - \beta[\sigma(N_1) + \sigma(N_2)]\} \quad (7)$$

schematized in **6**; α and β are the mixing coefficient of each

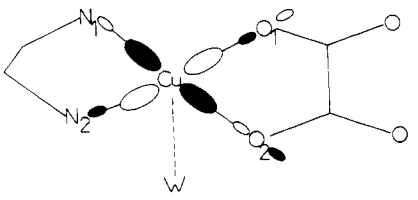

6

σ orbital of the bound oxygen and nitrogen atoms. This orbital is delocalized in the same plane as the oxalato ligand. On the contrary, in $dienCu(C_2O_4)\cdot 4H_2O$, the four nearest neighbors of the copper(II) are the three nitrogen atoms (N_1, N_2, N_3) of dien and only one of the oxygen atoms (O_1) of $C_2O_4^{2-}$, another oxygen atom occupying the apical position.[22] It follows that the unpaired electron, to a first approximation, is described by the orbital

$$\varphi = N\{d_{xy} - \alpha\sigma(O_1) - \beta[\sigma(N_1) + \sigma(N_2) + \sigma(N_3)]\} \quad (8)$$

schematized in **7**. This orbital is localized in a plane perpendicular to the plane of the oxalato ligand. As regards the orientation of the singly occupied orbital, a situation analogous to **7** can be obtained by starting from $tmenCu(C_2O_4)\cdot 4H_2O$ and by fixing a new nitrogen-containing ligand L that reverses the orientation of the orbital as shown in **8**. In both **7** and

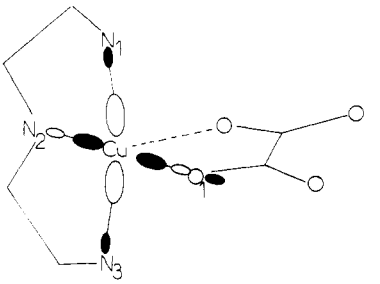

7

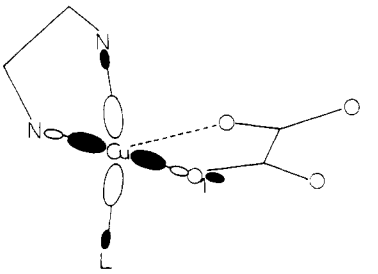

8

8, owing to the admixture of some d_{z^2} metal orbital in the singly occupied orbital of the CuN_3O_2 chromophore of low symmetry, there can also be a small spin density on the oxygen atom occupying the apical position.

Finally, Hendrickson showed that, by replacing dien in **7** by petdien (=*N*,*N*,*N'*,*N''*,*N''*-pentaethyldiethylenetriamine), one increases the trigonal character of the CuN_3O_2 chromophore, with a significant admixture of the d_{z^2} metal orbital in the singly occupied orbital.[23] In the borderline case of a genuine trigonal-bipyramidal symmetry with a N_1CuO_1 axis and a $N_2N_3O_2$ equatorial plane, the singly occupied orbital would be

$$\varphi = N\{d_{z^2} - (3^{-1/2})\alpha[2\sigma(O_1) - \sigma(O_2)] - (3^{-1/2})\beta[2\sigma(N_1) - \sigma(N_2) - \sigma(N_3)]\} \quad (9)$$

as schematized in **9**. z refers to the pseudo-trigonal axis.

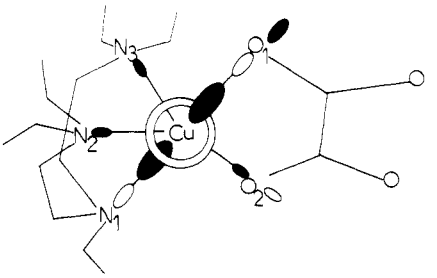

9

6 represents each of the monomeric fragments of the complex $[tmen(H_2O)Cu(C_2O_4)Cu(H_2O)tmen]^{2+}$, and the orbital drawn in **6** may be considered as one of the two magnetic orbitals of the binuclear system. This complex was first reported by Nonoyama.[24] These magnetic orbitals are properly

(19) Julve, M.; Verdaguer, M.; Charlot, M. F.; Kahn, O.; Claude, R. *Inorg. Chim. Acta* **1984**, *82*, 5–12.
(20) Gazo, J.; Bersuker, I. B.; Garaj, J.; Kabesova, M.; Kohout, J.; Langfelderova, H.; Melnik, M.; Serator, M.; Valach, F. *Coord. Chem. Rev.* **1976**, *19*, 253–297.
(21) Korvenranta, J. *Suom. Kemistil. B* **1973**, *46*, 296–301.
(22) Stephens, F. S. *J. Chem. Soc. A* **1969**, 2493–2501.
(23) Felthouse, T. R.; Laskowski, E. J.; Hendrickson, D. N. *Inorg. Chem.* **1977**, *16*, 1077–1089.
(24) Nonoyama, K.; Ojima, H.; Ohki, K.; Nonoyama, N. *Inorg. Chim. Acta* **1980**, *41*, 155–159.
(25) Curtis, N. F.; McCormick, I. R. N.; Waters, T. N. *J. Chem. Soc., Dalton Trans.* **1973**, 1537–1548.

oriented to interact on either side of the bridge owing to the overlaps between the σ orbitals of the oxygen atoms bound to a same carbon atom of the oxalato bridge. If we put $s = \langle\sigma(O)|\sigma(O')\rangle$ for the overlap shown in **10**, then, from (7), the overlap integral between the two magnetic orbitals may be approximated by $S_1 = 2\alpha^2 s$.

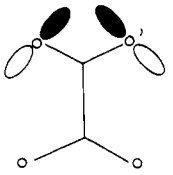

10

7 represents each of the monomeric fragments of $[(dien)Cu(C_2O_4)Cu(dien)]^{2+}$, and, as above, the orbital drawn in **7** may be considered as one of the two magnetic orbitals of the binuclear complex. The two short Cu–O bonds must be trans with regard to the C–C bond of $C_2O_4^{2-}$. It follows that the two magnetic orbitals are unfavorably oriented to interact, and in the absence of d_{z^2} admixture, the overlap integral may be estimated as zero. In case there should be some d_{z^2} admixture, owing to the residual spin density on the oxygen atoms in apical positions, the overlap may be slightly different from zero. In an identical way, one sees from (8) that the overlap integral between the magnetic orbitals in $[tmen(L)Cu(C_2O_4)Cu(L)tmen]^{2+}$ is close to zero.

The two magnetic orbitals in the dissymmetrical binuclear complex $[(dien)Cu(C_2O_4)Cu(tmen)]^{2+}$ are represented in **7** and **6**, respectively. Owing to the relative orientations of these magnetic orbitals, the interaction occurs only on one side of the bridge and the overlap may be approximated to $S_2 = \alpha^2 s$.

Finally, in a hypothetical binuclear complex for which **9** would represent each of the two monomeric fragments, the overlap integral between the magnetic orbitals, from (9), would be $S_3 = 4\sigma^2 s/3$.

In summation and on the assumption that J varies as the square of the overlap integral between the magnetic orbitals, our predictions concerning the relative magnitudes of the antiferromagnetic interaction in a series of μ-oxalato copper(II) binuclear complexes are as follows:

(i) In $[tmen(H_2O)Cu(C_2O_4)Cu(H_2O)tmen]^{2+}$, in spite of the large separation between the metal centers, the interaction is expected to be strongly antiferromagnetic with $J = J_1$.

(ii) In $[(dien)Cu(C_2O_4)Cu(dien)]^{2+}$ and $[tmen(L)Cu(C_2O_4)Cu(L)tmen]^{2+}$, the interaction is expected to be either negligible or very small.

(iii) In $[(dien)Cu(C_2O_4)Cu(tmen)]^{2+}$, the interaction is expected to be of intermediate magnitude with J_2 close to $J_1 S_2^2/S_1^2$, i.e. $J_1/4$.

(iv) In a $[N_3Cu(C_2O_4)CuN_3]^{2+}$ complex, in which N_3 symbolizes a tridentate nitrogen ligand, the interaction is expected to be smaller than $J_1 S_3^2/S_1^2$, i.e. $4J_1/9$, this limit corresponding to hypothetical purely trigonal-bipyramidal surroundings with NCuO axes.

Description of the Structures

$[tmen(H_2O)Cu(C_2O_4)Cu(H_2O)tmen](ClO_4)_2 \cdot 1.25H_2O$ (1). The structure is made up of two kinds of centrosymmetric, crystallographically independent but almost identical binuclear cations, isolated by noncoordinated ClO_4^- anions and inserted water molecules. Two perspective views of one of the cations are shown in Figure 2. The crystal packing is shown in Figure 3. Selected bond lengths and angles are given in Table I. The environment of each copper(II) ion is square pyramidal with a water molecule in the apical position, the Cu–O distances being 2.364 (5) and 2.312 (5) Å, respectively, and the displacement of the metal atom from the N(1)N(2)O(1)O(2) mean basal plane toward the water molecule being 0.147 (1) and 0.182 (1) Å. For this and the two other structures, the Muetterties and Guggenberger dihedral angle criterion was used to visualize deviations from ideal coordination geometries.[26] The dihedrals were calculated according to Kouba

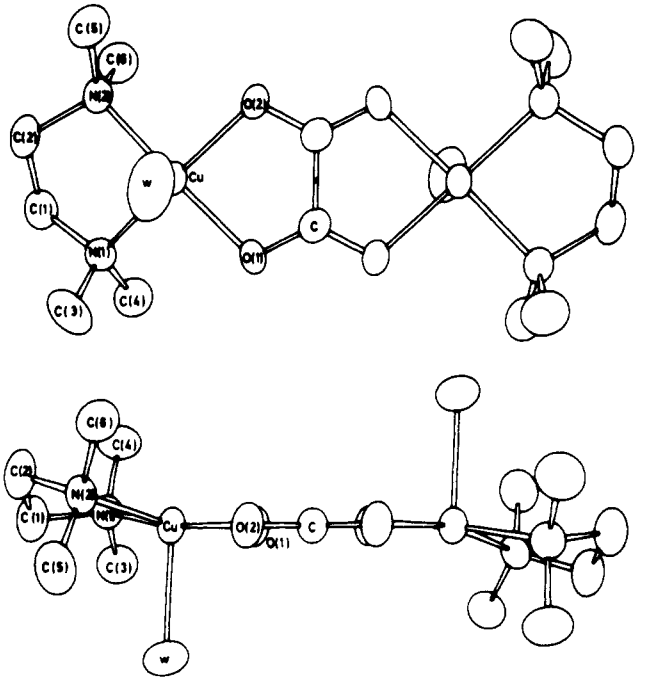

Figure 2. Perspective views of one of the binuclear cations $[tmen(H_2O)Cu(C_2O_4)Cu(H_2O)tmen]^{2+}$.

Table I. Selected Bond Lengths (Å) and Angles (deg) in $[tmen(H_2O)Cu(C_2O_4)Cu(H_2O)tmen](ClO_4)_2 \cdot 1.25H_2O$ (1)[a]

	unit 1	unit 2
Cu Environment		
Cu-O(1)	1.977 (4)	1.980 (4)
Cu-O(2)	1.977 (4)	1.975 (4)
Cu-N(1)	2.011 (5)	2.008 (5)
Cu-N(2)	2.005 (5)	2.010 (5)
Cu-OW	2.364 (5)	2.312 (5)
Cu···Cu^i	5.147 (2)	5.167 (2)
OW-Cu-O(1)	87.5 (2)	91.5 (2)
OW-Cu-O(2)	91.1 (2)	91.6 (2)
OW-Cu-N(1)	101.6 (2)	95.5 (2)
OW-Cu-N(2)	96.6 (2)	102.2 (2)
O(1)-Cu-O(2)	84.5 (2)	84.0 (2)
O(1)-Cu-N(1)	93.8 (2)	94.0 (2)
O(1)-Cu-N(2)	175.4 (2)	166.0 (2)
O(2)-Cu-N(1)	167.2 (2)	172.8 (2)
O(2)-Cu-N(2)	93.2 (2)	92.6 (2)
N(1)-Cu-N(2)	87.5 (2)	87.6 (2)
Oxalato Bridge		
C-O(1)	1.235 (7)	1.238 (7)
C^i-O(2)	1.246 (7)	1.251 (7)
C-C^i	1.56 (1)	1.54 (1)
Cu-O(1)-C	111.3 (2)	111.4 (2)
Cu-O(2)-C^i	111.6 (2)	111.8 (2)
O(1)-C-C^i	116.9 (7)	117.1 (7)
O(2)-C^i-C	115.5 (7)	115.8 (7)
O(1)-C-O(2)^i	127.6 (6)	127.1 (6)
Intermolecular Bonds		
O(1)p(1)-OW(3)^{ii}	2.886 (9)	O(2)p(2)-OW(2)^{iii} 2.79 (2)
O(2)p(1)-OW(1)	2.772 (9)	O(7)p(2)-OW(2)^{iii} 2.85 (2)
OW(3)-OW(2)	2.797 (7)	O(7)p(2)-OW(4) 2.82 (3)

[a] Roman numeral superscripts refer to the following equivalent positions relative to x, y, z: (i) $\bar{x}, \bar{y}, \bar{z}$ in unit 1 and $^1/_2 - x, ^1/_2 - y, \bar{z}$ in unit 2; (ii) $x, y, 1 + z$; (iii) $x, 1 - y, z$.

(26) Muetterties, E. L.; Guggenberger, L. J. *J. Am. Chem. Soc.* **1974**, *96*, 1748–1756.

Table II. Comparison of Cu Environments in Compounds **1-3** and in $[(dien)Cu(C_2O_4)Cu(dien)](ClO_4)_2$ (4) and $[(petdien)Cu(C_2O_4)Cu(petdien)](BPh_4)_2$ (5) according to the Dihedral Angle Criterion[a]

di-hedral	square pyramid	1		4[25]		2	3	5[23]	trigonal bipyramid	tetra-hedron	2	square planar
		Cu(1)	Cu(2)	Cu(1)	Cu(2)	dien side					tmen side	
δa_1	119.8	125.2	124.4	126.0	123.6	125.8	107.8	116.9	101.5	109.5	167.6	180
		N(2)-N(1)	N(1)-N(2)	N(1)-N(3)	N(5)-N(4)	N(2)-N(3)	O(2)-N(3)	N(1)-N(2)			O(4)-N(5)	
δa_2	75.7	74.6	76.0	66.0	70.5	68.9	86.5	100.0	101.5	109.5	168.8	180
		N(2)-OW	N(1)-OW	N(2)-O(9)	N(5)-O(11)	N(2)-O(1)	O(2)-O(1)	N(1)-N(3)			N(5)-N(1)	
δa_3	119.8	119.0	117.8	126.1	121.0	121.9	110.0	91.2	101.5	109.5	16.8	0
		N(2)-O(2)	N(1)-O(1)	N(2)-N(1)	N(5)-N(6)	N(2)-N(4)	O(2)-N(2)	N(1)-O(2)			N(5)-O(3)	
δa_4	119.8	119.8	121.4	114.4	114.9	116.3	113.1	113.8	101.5	109.5	168.3	180
		O(1)-N(1)	O(2)-N(2)	O(10)-N(3)	O(12)-N(4)	O(2)-N(3)	N(1)-N(3)	O(1)-N(2)			O(3)-O(4)	
δa_5	75.7	76.8	74.9	86.4	87.8	87.4	83.0	91.6	101.5	109.5	16.7	0
		O(1)-OW	O(2)-OW	O(10)-O(9)	O(12)-O(11)	O(2)-O(1)	N(1)-O(1)	O(1)-N(3)			N(1)-O(4)	
δa_6	119.8	117.2	118.5	112.6	109.1	108.5	118.2	101.3	101.5	109.5	167.9	180
		O(1)-O(2)	O(2)-O(1)	O(10)-N(1)	O(12)-N(6)	O(2)-N(4)	N(1)-N(2)	O(1)-O(2)			N(1)-O(3)	
δe_1	75.7	67.8	68.5	67.4	64.2	61.0	65.5	45.7	53.1			
		N(1)-OW	N(2)-OW	N(3)-O(9)	N(4)-O(11)	O(1)-N(3)	O(1)-N(3)	N(2)-N(3)				
δe_2	75.7	70.8	72.3	69.4	70.0	69.3	58.3	68.2	53.1			
		O(2)-OW	O(1)-OW	N(1)-O(9)	N(6)-O(11)	O(1)-N(4)	O(1)-N(2)	O(2)-N(3)				
δe_3	0	8.5	6.6	11.9	16.8	18.5	30.2	42.9	53.1			
		N(1)-O(2)	N(2)-O(1)	N(3)-N(1)	N(4)-N(6)	N(3)-N(4)	N(2)-N(3)	N(2)-O(2)				
Δ	1	0.93	0.95	0.90	0.79	0.80	0.54	0.21	0	1	0.16	0

[a] Δ is the distortion parameter proposed by Galy et al.[35] For 5-coordination: $\Delta = [\delta a_1 + \delta a_3 + \delta a_4 + \delta a_6 - 406]/164.7 + [\delta e_1 + \delta e_2 - 106.2]/203.4 + [203 - \delta a_2 - \delta a_5]/232.2 + [53.1 - \delta e_3]/477.9$. For 4-coordination: $\Delta = [720 - \delta a_1 - \delta a_2 - \delta a_4 - \delta a_6]/423 + (\delta a_3 + \delta a_5)/657$. The numbering scheme for dihedrals is the same as in ref 26.

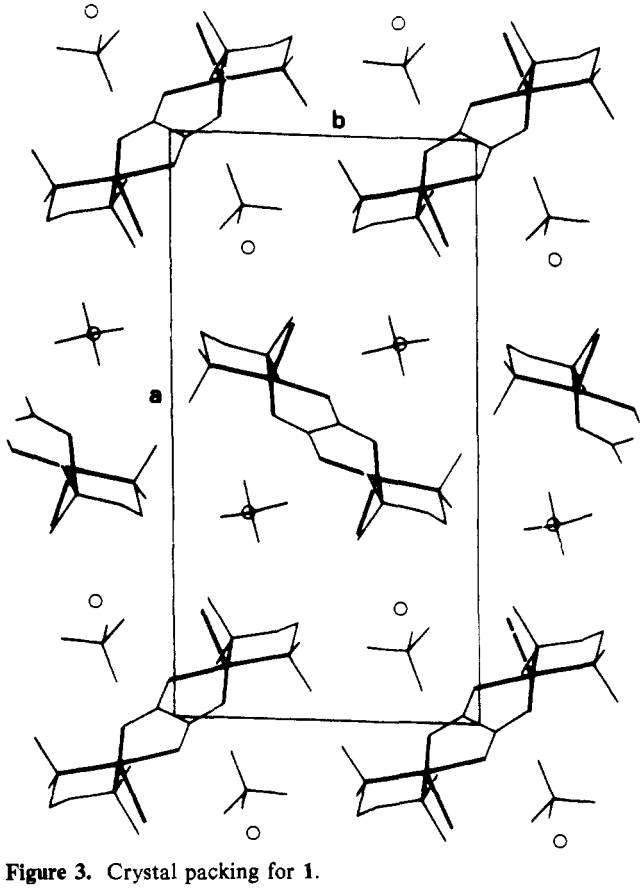

Figure 3. Crystal packing for **1**.

and Wreford's model for systems with inequivalent ligands.[27] They are listed in Table II, as well as the values corresponding to idealized polyhedra: in both binuclear units of **1** the copper environment does not deviate much from the ideal square pyramid. The centrosymmetrical $Cu(C_2O_4)Cu$ networks have a flattened-chair configuration: each $C_2O_4^{2-}$ anion is planar with atom-to-plane distances less than 0.007 (6) Å; the distances between the Cu(II) ions and the oxalato planes are 0.146 (1) Å for Cu(1) and only 0.023 (1) Å for Cu(2). The

(27) Kouba, J. K.; Wreford, S. S. *Inorg. Chem.* **1976**, *15*, 1463-1465.

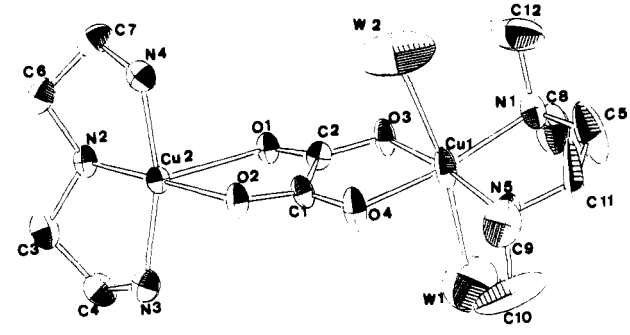

Figure 4. Perspective view of the binuclear cation $[dienCu(C_2O_4)Cu(H_2O)_2tmen]^{2+}$.

Cu-O bond lengths are nearly equal (1.98 Å) and so are the Cu-N bond lengths (2.01 Å). The C-O bond lengths range from 1.235 (7) to 1.251 (7) Å and do not differ significantly. The length of the C-C bond in $C_2O_4^{2-}$ is typical of a single bond: 1.56 (1) and 1.54 (1) Å. The intramolecular Cu···Cu separations are 5.147 (2) and 5.167 (1) Å while the shortest intermolecular Cu···Cu distance amounts to 7 Å.

Examination of the distances between the oxygen atoms and the positions of known H atoms shows that each ClO_4^- anion is weakly bonded to two water molecules, one coordinated to a Cu atom (W(1) or W(2)) and the other one inserted (W(3) or W(4)). Only one of the two ClO_4^- anions, p(2), is disordered, with two arrangements sharing the bond Cl(2)-O(1)-p(2). This is related to the fact that the corresponding inserted water molecule W(4), contrary to the other one, W(3), is not bonded to one of the coordinated water molecules and is only statistically distributed in the structure.

$[dienCu(C_2O_4)Cu(H_2O)_2tmen](ClO_4)$ (2). The structure is made up of dissymmetrical binuclear cations and noncoordinated perchlorate anions. Figure 4 gives a perspective view of the cation. The crystal packing is represented in Figure 5. Selected bond lengths and angles are listed in Table III.

On the tmen side, the Cu(II) ion is in a 4 + 2 surrounding. The four nearest neighbors are the nitrogen atoms of tmen and two oxygen atoms of the oxalato bridge: Cu(1)-O(3) = 1.954 (6) Å, Cu(1)-O(4) = 1.969 (6) Å. They are located at the corners of a rather flattened tetrahedron (Table II). The two apical positions are occupied by water molecules with Cu(1)-OW(1) = 2.62 (1) Å and Cu(1)-OW(2) = 2.72 (1) Å.

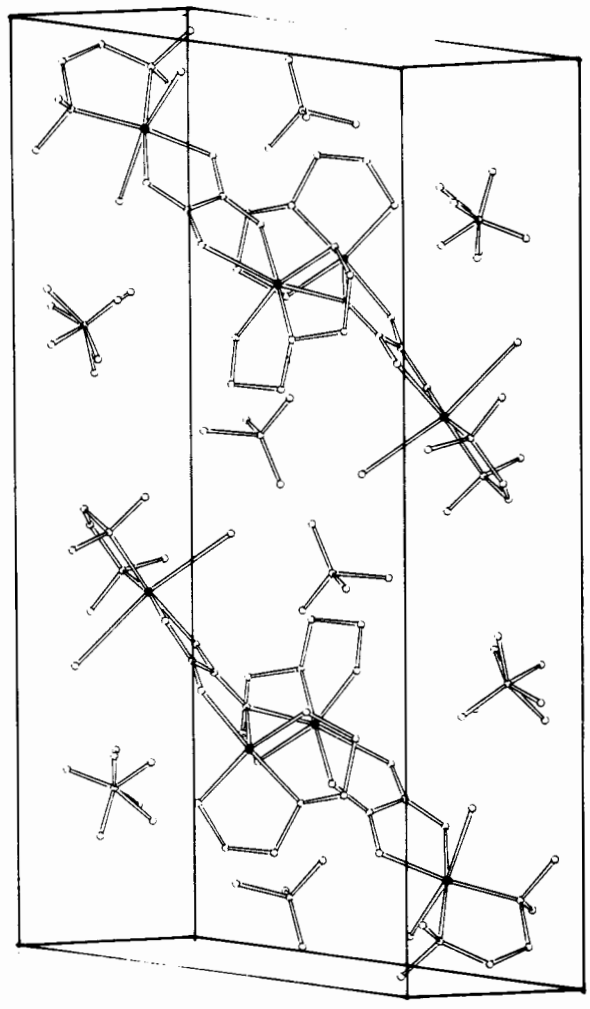

Figure 5. Crystal packing for **2**.

On the dien side, the Cu(II) ion is again in a 4 + 2 environment. The four nearest neighbors are the three nitrogen atoms of dien and an oxygen atom of the oxalato bridge: Cu(2)–O(2) = 1.969 (5) Å. They occupy the basal corners of a square pyramid whose apex is occupied by a second oxygen atom of $C_2O_4^{2-}$: Cu(2)–O(1) = 2.461 (5) Å. As shown in Table II the distortion toward trigonal bipyramidal is more important than in compound **1**. An oxygen atom $O(1)^i$ belonging to the oxalato bridge of a neighboring cationic unit stands opposite O(1) at 2.752 (5) Å from Cu(2). Owing to this Cu(2)–$O(1)^i$ interaction the binuclear cations form chains parallel to the *b* axis, as shown in Figure 5. The $Cu(C_2O_4)Cu$ network significantly deviates from the planarity. The Cu···Cu separation through the oxalato bridge inside the binuclear cation is 5.399 (2) Å, but the shortest Cu···Cu separation is observed between copper(II) ions belonging to two different cations, weakly bound to the same $O(1)^i$ oxygen atom. This separation is Cu(2)···$Cu(2)^i$ = 4.628 (1) Å. The third short Cu···Cu distance, equal to 5.844 (2) Å, is observed between Cu(1) and $Cu(2)^i$.

One of the perchlorate anions is strongly disordered, with the oxygen atoms occupying seven sites. For the second perchlorate anion, the disorder is much weaker and we neglected it.

[tmen(2-MeIm)Cu(C_2O_4)Cu(2-MeIm)tmen](PF_6)$_2$ (3). The structure is made up of centrosymmetrical binuclear cations and uncoordinated PF_6^- anions. Figure 6 gives two perspective views of the cation and Figure 7 represents the crystal packing. Selected bond lengths and angles are given in Table IV. The environment around each copper(II) ion is intermediate between the square pyramid and the trigonal bipyramid as shown by the dihedrals listed in Table II. A square-pyramid description places the two nitrogen atoms of tmen, N(1) and N(2), one of the nitrogen atoms of 2-MeIm, N(3), and one of the oxgen atoms of the oxalato bridge, O(2), in the basal plane, the other oxalato oxygen atom, O(1), occupying the apical position. The Cu(II)–ligand distances in the basal plane, from 1.991 to 2.056 Å, are significantly shorter than the apical bond length Cu–O(1) = 2.208 (2) Å. The angles around Cu(II) in the basal plane vary from 86.6 to 96.1 (1)°. The

Table III. Selected Bond Lengths (Å) and Angles (deg) in [dienCu(C_2O_4)Cu(H_2O)$_2$tmen](ClO_4)$_2$ (**2**)[a]

	Cu(1) Environment		
Cu(1)–N(1)	2.001 (7)	Cu(1)–O(4)	1.969 (6)
Cu(1)–N(5)	2.008 (8)	Cu(1)–OW(1)	2.62 (1)
Cu(1)–O(3)	1.954 (6)	Cu(1)–OW(2)	2.72 (1)
O(3)–Cu(1)–O(4)	84.1 (2)	O(4)–Cu(1)–N(5)	92.2 (3)
O(3)–Cu(1)–N(1)	95.6 (3)	N(1)–Cu(1)–N(5)	88.8 (3)
	Cu(2) Environment		
Cu(2)–O(1)	2.461 (5)	Cu(2)–N(3)	1.977 (7)
Cu(2)–O(2)	1.969 (5)	Cu(2)–N(4)	2.004 (7)
Cu(2)–N(2)	1.975 (7)	Cu(2)–$O(1)^i$	2.752 (5)
O(2)–Cu(2)–N(4)	98.1 (3)	N(4)–Cu(2)–O(1)	92.9 (2)
O(2)–Cu(2)–N(3)	93.3 (3)	N(4)–Cu(2)–$O(1)^i$	83.3 (2)
O(2)–Cu(2)–O(1)	75.1 (3)	O(2)–Cu(2)–$O(1)^i$	90.0 (2)
N(2)–Cu(2)–N(3)	85.0 (3)	N(2)–Cu(2)–$O(1)^i$	104.3 (2)
N(2)–Cu(2)–N(4)	84.7 (3)	N(3)–Cu(2)–$O(1)^i$	85.9 (2)
N(2)–Cu(2)–O(1)	99.8 (2)	O(1)–Cu(2)–$O(1)^i$	155.1 (1)
N(3)–Cu(2)–O(1)	102.3 (2)		
	Oxalato Bridge		
O(4)–C(1)	1.26 (1)	C(1)–O(2)	1.26 (1)
O(3)–C(2)	1.270 (9)	C(2)–O(1)	1.233 (9)
C(1)–C(2)	1.53 (1)		
Cu(2)–O(1)–C(2)	106.1 (4)	O(4)–C(1)–C(2)	117.5 (7)
Cu(2)–O(2)–C(1)	120.5 (5)	O(2)–C(1)–C(2)	119.9 (7)
Cu(1)–O(3)–C(2)	112.9 (4)	O(1)–C(2)–C(1)	117.5 (7)
Cu(1)–O(4)–C(1)	110.5 (5)	O(1)–C(2)–O(3)	128.6 (7)
O(2)–C(1)–O(4)	122.6 (7)	O(3)–C(2)–C(1)	113.9 (7)
	Cu–Cu Distances		
Cu(1)–Cu(2)	5.399 (2)	Cu(1)–$Cu(2)^i$	5.844 (2)
Cu(2)–$Cu(2)^i$	4.628 (1)		

[a] Roman superscript i refers to equivalent position $\bar{x}$, $^1/_2 + y$, $^1/_2 - z$.

Table IV. Selected Bond Lengths (Å) and Angles in [tmen(2-MeIm)Cu(C_2O_4)Cu(2-MeIm)tmen](PF_6)$_2$ (**3**)[a]

	Cu Environment		
Cu–O(1)	2.208 (2)	Cu–N(2)	2.056 (2)
Cu–O(2)	1.997 (2)	Cu–N(3)	1.991 (2)
Cu–N(1)	2.025 (2)	Cu–Cu^i	5.434 (2)
O(1)–Cu–O(2)	79.64 (7)	O(2)–Cu–N(2)	90.43 (9)
O(1)–Cu–N(1)	96.82 (9)	O(2)–Cu–N(3)	88.66 (9)
O(1)–Cu–N(2)	105.92 (8)	N(1)–Cu–N(2)	86.6 (1)
O(1)–Cu–N(3)	100.88 (8)	N(1)–Cu–N(3)	96.1 (1)
O(2)–Cu–N(1)	174.57 (8)	N(2)–Cu–N(3)	152.56 (9)
	Oxalato Bridge		
C(1)–O(1)	1.241 (3)	C(1)–$C(1)^i$	1.562 (4)
$C(1)^i$–O(2)	1.250 (3)		
Cu–O(1)–C(1)	109.5 (1)	O(2)–$C(1)^i$–C(1)	117.1 (2)
Cu–O(2)–$C(1)^i$	116.0 (1)	O(1)–C(1)–$O(2)^i$	125.7 (2)
O(1)–C(1)–$C(1)^i$	117.1 (1)		
	2-Methylimidazole Ligand		
N(3)–C(8)	1.326 (3)	C(9)–C(10)	1.346 (5)
C(8)–N(4)	1.335 (4)	C(10)–N(3)	1.376 (4)
N(4)–C(9)	1.349 (5)	C(8)–C(11)	1.460 (5)
Cu–N(3)–C(8)	123.3 (2)	N(3)–C(8)–N(4)	109.4 (3)
Cu–N(3)–C(10)	129.2 (2)	C(8)–N(4)–C(9)	108.4 (3)
C(8)–N(3)–C(10)	106.8 (2)	N(4)–C(9)–C(10)	107.2 (3)
N(3)–C(8)–C(11)	125.9 (3)	C(9)–C(10)–N(3)	108.0 (3)
N(4)–C(8)–C(11)	124.7 (3)		

[a] Roman superscript i refers to equivalent position $\bar{x}$, $\bar{y}$, $\bar{z}$.

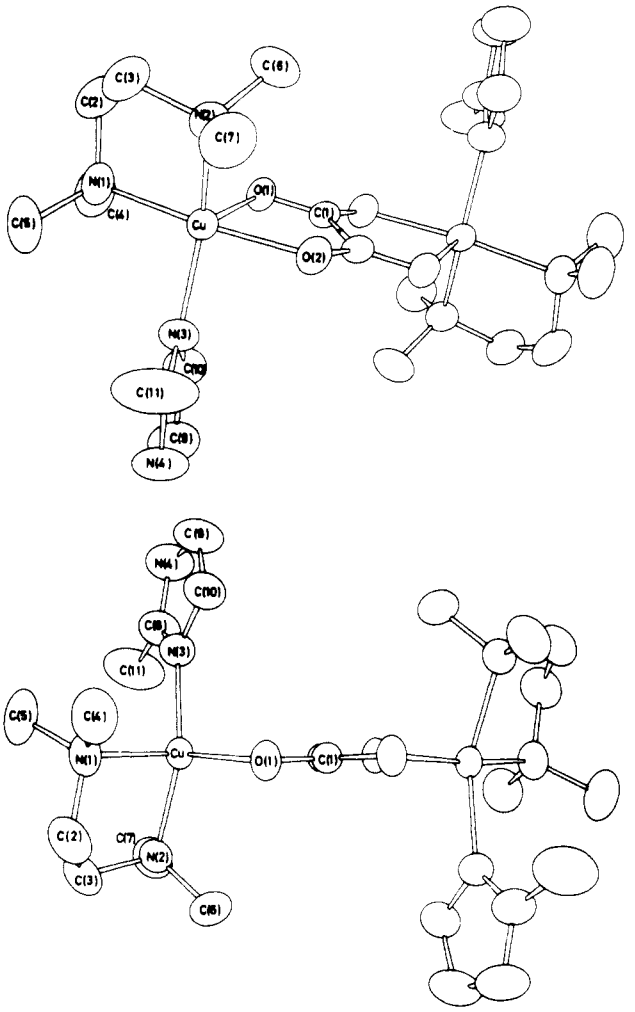

Figure 6. Perspective views of the binuclear cation [tmen(2-MeIm)Cu(C_2O_4)Cu(2-MeIm)tmen]$^{2+}$.

metal is displaced by 0.184 (1) Å from the mean basal plane toward the apex O(1). A trigonal-bipyramid description places N(2), N(3), and O(1) in the equatorial plane and N(1) and O(2) in axial positions. Cu(II) deviates by only 0.084 (1) Å from this equatorial plane and the pseudo-trigonal axis does not show too much distortion from linearity, N(1)–Cu–O(2) being 174.57 (8)°. However, the angles in the equatorial plane depart significantly from the theoretical 120° value, with values of 100.88 (8), 105.92 (8), and 152.56 (9)°.

The comparison between the environments of the copper(II) ion in **3** and in other μ-oxalato copper(II) complexes in which the metal is surrounded by three nitrogen and two oxygen atoms shows that the trend toward the trigonal bipyramid, as estimated by the distortion parameter Δ defined in Table II, increases according to the dien side of **2** ~ [(dien)Cu(C_2O_4)Cu(dien)](ClO_4)$_2$[25] < **3** < [(petdien)Cu(C_2O_4)Cu(petdien)](BPh_4)$_2$.[23]

As in compound **1** the centrosymmetrical C_2O_4 bridge is planar with atom-to-plane distances not exceeding 0.001 (2) Å. The Cu(II) ions on each side are ±0.185 (1) Å from the bridge plane, giving the Cu(C_2O_4)Cu network a flattened-chair configuration.

The 2-methylimidazole ligand is almost planar with atom-to-plane distances less than 0.030 (6) Å and a Cu-to-plane distance equal to 0.194 (1) Å. The angle between oxalato and 2-methylimidazole mean planes is 78.9 (1)°.

The intramolecular Cu···Cu separation amounts of 5.434 (2) Å. The shortest intermolecular Cu···Cu distance is 7.5 Å.

The PF_6^- anion presents two orientations around the pseudo-fourfold axis F(1)–P–F(2).

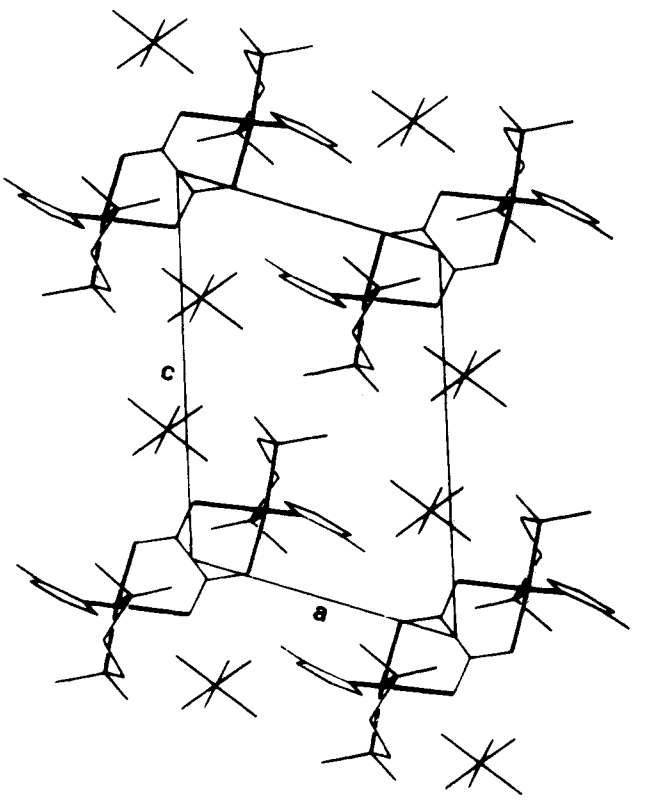

Figure 7. Crystal packing for **3**.

Magnetic Properties and S–T Energy Gaps in 1–3

The interaction in the binuclear complexes **1–3** leads to spin-singlet and spin-triplet low-lying states separated by J, of which the value can be deduced from the temperature dependence of the molar magnetic susceptibility χ_M of the binuclear unit, expressed according to

$$\chi_M = \frac{2N\beta^2g^2}{kT}\left|3 + \exp\left(-\frac{J}{kT}\right)\right|^{-1} + 2N\alpha \qquad (10)$$

where the symbols have their usual meaning. In the case of the dissymmetrical complex **2**, a very small additional term arising from the coupling of the $M_s = 0$ components of the singlet and the triplet occurs in the expression of χ_M.[28] It was shown that, when $|J|$ is sufficiently large (>10 cm^{-1}), the influence of this term is negligible.[17] Whatever the care in the synthesis of the compounds may be, the samples always contain some noncoupled species giving a Curie tail at very low temperature. To account for this, the experimental susceptibility χ_M^{exptl} is expressed as

$$\chi_M^{exptl} = \chi_M(1 - \rho) + \rho\frac{C}{T} \qquad (11)$$

where ρ is the mass proportion of noncoupled impurity assumed to follow a Curie law. If the molecular weight of the impurity is assumed to be equal to that of the coupled compound, C is equal to $N\beta^2g^2/2k$. In the fitting of the magnetic data, we use this value of C.

The magnetic properties of **1–3** are given in Figure 8. The three curves exhibit a behavior characteristic of antiferromagnetically coupled copper(II) pairs with a rounded maximum in the susceptibility occurring at about 300 K for **1**, at 62 K for **2**, and 10.8 K for **3**. Least-squares fittings of the experimental data using relation 11 lead to the parameters given in Table V. In **1**, the interaction is very large with J_1

(28) Barraclough, C. G.; Brookes, R. W.; Martin, R. L. *Aust. J. Chem.* **1974**, *27*, 1843–1850.

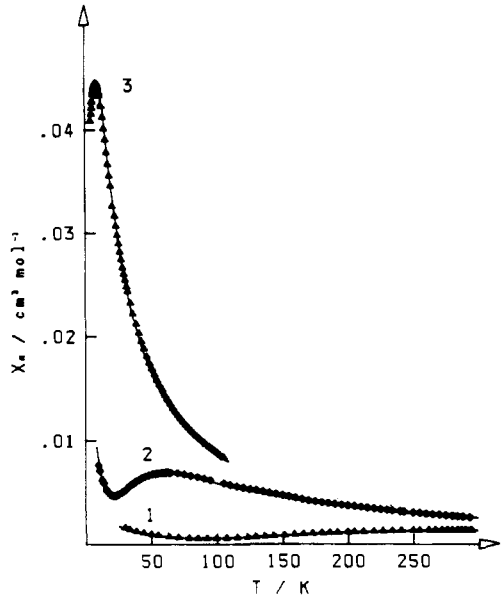

Figure 8. Experimental and calculated magnetic data for **1**–**3**.

Table V. Parameters Deduced from the Magnetic Data

	J, cm^{-1}	g	ρ	10^4R^b
1	−385.4	2.16 (7)	0.0509	3.89
2	−75.5	2.12 (4)	0.0914[a]	2.34
3	−13.8	2.08 (1)	0.034	5.22

[a] The unusually large value of ρ for **2** comes from the fact that the sample contained a small proportion of the symmetrical complex $[(dien)Cu(C_2O_4)Cu(dien)](ClO_4)_2$, for which J was found close to zero. [b] R is the agreement factor defined as $\Sigma|\chi_M^{obsd} - \chi_M^{calcd}|^2/\Sigma(\chi_M^{obsd})^2$.

= −385.4 cm^{-1}. In **2**, it is of medium magnitude with J_2 = −75.5 cm^{-1}, and in **3**, it is much smaller with J_3 = −13.8 cm^{-1}.

Discussion and Perspectives

In addition to compounds **1**–**3**, we include in the discussion the compounds $[(dien)Cu(C_2O_4)Cu(dien)]X_2$ and $[(petdien)Cu(C_2O_4)Cu(petdien)]X_2$, where X^- is a counteranion. For $X = ClO_4$, J is found negligible in the former compound and equal to −19.6 cm^{-1} in the latter.[25] When ClO_4^- is replaced by BPh_4^- as the counteranion, J in the petdien compound reaches −74.8 cm^{-1}. The crystal structures of both $[(dien)Cu(C_2O_4)Cu(dien)](ClO_4)_2$[25] and $[(petdien)Cu(C_2O_4)Cu(petdien)](BPh_4)_2$[23] were refined. To begin with, we wish to compare the experimental results with the predictions established in the third section:

(i) As expected, owing to the favorable orientation of the magnetic orbitals, **1** exhibits a strong antiferromagnetic interaction characterized by J_1 = −385.4 cm^{-1}.

(ii) Again as expected, the interaction in $[(dien)Cu(C_2O_4)Cu(dien)](ClO_4)_2$ is negligible.

(iii) The interaction in **3** is much weaker than in **1**, due to the reversal of the magnetic orbitals by fixation of the 2-MeIm ligands. This interaction, however, is not zero (J_3 = −13.8 cm^{-1}). The low symmetry of the CuN_3O_2 chromophore allows a weak delocalization of each magnetic orbital on the oxygen atom of the oxalato bridge 2.208 Å from the copper atom. It was shown above that in **3** the trigonal-bipyramidal character is more pronounced than in $[(dien)Cu(C_2O_4)Cu(dien)](ClO_4)_2$ and less pronounced than in $[(petdien)Cu(C_2O_4)Cu(petdien)](BPh_4)_2$. The relative magnitudes of the interaction in these three compounds reflect this structural trend.

(iv) The ratio J_1/J_2 is about 5 whereas we expected a ratio of 4. In this respect, we can notice that the environment of the dien side of **2** has nearly no trigonal-bipyramidal character with a very long apical bond length (2.461 Å). As a result the delocalization of the magnetic orbital on this apical site is actually negligible.

(v) $[(petdien)Cu(C_2O_4)Cu(petdien)](BPh_4)_2$ is the already reported μ-oxalato copper(II) complex in which the environment of the metal has the most pronounced trigonal-bipyrmidal character.[23] We are, however, still far from purely trigonal-bipyramidal chromophores, and the S–T energy gap is much weaker than the predicted limit $4J_1/9$ = −171 cm^{-1}. The structure of $[(petdien)Cu(C_2O_4)Cu(petdien)](ClO_4)_2$ (J = −19.6 cm^{-1}) is not known but that of the PF_6^- derivative (J = −19.2 cm^{-1}) was recently reported.[36] It confirms that the trigonal-bipyramidal character is significantly less pronounced than in the BPh_4^- compound.

The encouraging agreement between predictions and experimental results must not hide the difficulties encountered in designing coupled systems with predictable magnetic properties. These difficulties are of two kinds, those related to the synthesis and those related to the theory of the phenomenon. Concerning the synthesis first, we can mention some of the unresolved problems:

(i) In **1**, the delocalization of each magnetic orbital toward the oxygen atoms of $C_2O_4^{2-}$ bound to the metal depends to some extent on the displacement of the metal from the basal plane. The larger this displacement is, the weaker the mixing coefficient α in (7) and the smaller the S–T energy gap. The enhancement of the interaction when the copper(II) ions are strictly in the basal plane was recently evidenced in bis(triketonato)copper(II) binuclear complexes.[29] By working in methanol instead of water, we prepared the fully dehydrated complex $[(tmen)Cu(C_2O_4)Cu(tmen)](ClO_4)_2$. Surprisingly, J is exactly the same as in **1**. We did not obtain single crystals, so that we do not know whether in this water-free complex the copper atoms are actually in the basal planes N_2O_2.

(ii) When reversing the magnetic orbitals by fixation of two nitrogen-containing ligands L on **1**, we cannot yet control the trigonal-bipyramidal character of the resulting compound. We know that this orbital reversal leads to a drastic decrease of the antiferromagnetic interaction. However, we are not able to predict whether J will be very close to zero or be of the order of −10 cm^{-1}.

(iii) An important aspect of this work is the synthesis of dissymmetrical complexes like **2**. Unfortunately, we were not able to prepare $[(petdien)Cu(C_2O_4)Cu(tmen)]^{2+}$, for which we could predict a J value of the order of −150 cm^{-1}. More generally, the synthesis is likely the limiting step of this molecular engineering.

Concerning now the theoretical aspect of this work, we wish to point out briefly the unresolved problems:

(i) The basic model of the exchange interaction that we used is based on the approximation of the active electrons. This approximation underestimates the role of the low-energy doubly occupied MO's.[2,3] It can even lose its validity when some of these MO's are close in energy to the magnetic orbitals. The spin-polarization effects can then become preponderant.[30,31]

(ii) In expressions 7–9, the delocalization of the singly occupied orbitals toward the oxygen atoms is described in a quite simplified way. It is implicitly assumed that the basal Cu–O distances in the square-pyramidal environments and the axial and equatorial Cu–O distances in the trigonal-bipyramidal environments are all equal. Thus, the ratio J_1/J_2 = 4 has to be considered as a rough estimation.

(29) Wishart, J. F.; Ceccarelli, C.; Lintvedt, L.; Berg, J. M.; Foley, D. P.; Frey, T.; Hahn, J. E.; Hodgson, K. O.; Weis, R. *Inorg. Chem.* **1983**, *22*, 1667–1671.
(30) De Loth, P.; Cassoux, P.; Daudey, J. P.; Malrieu, J. P. *J. Am. Chem. Soc.* **1981**, *103*, 4007–4016.
(31) Kahn, O.; Sikorav, S.; Jeannin, S.; Jeannin, Y.; Goutheron, J. *Inorg. Chem.* **1983**, *22*, 2878–2883.

(iii) The last but not the least problem deals with the ferromagnetic contribution J_F. We assumed that in most of the coupled systems with extended bridging ligands, J_F was actually very small. For **1**, an ab initio calculation of the S–T splitting was performed.[32] Its results essentially confirm our own interpretation of the strong interaction, based on the overlaps between the oxygen atoms of the bridge bound to a same carbon atom. On one point, nevertheless, there is an apparent contradiction. In the ab initio calculation, the positive term J_F was found equal to 720 cm^{-1}. To understand this difference, one must realize that the two definitions of J_F are not equivalent.[33] In the ab initio calculation, J_F is calculated by using *orthogonal magnetic orbitals* ϕ'_A and ϕ'_B according to

$$J_F = 2j' \tag{12}$$

$$j' = \langle \phi'_A(1)\ \phi'_B(2)|r_{12}^{-1}|\phi'_A(2)\ \phi'_B(1)\rangle \tag{13}$$

Each orthogonal magnetic orbital may have a large residual contribution around the metal on which it is not centered.[33] More precisely, the larger the overlap S between nonorthogonal magnetic orbital is, the more important this residual contribution of ϕ'_A around B (and of ϕ'_B around A). It follows that j' as defined in (13) is expected to be much larger than j as defined in (4). This is particularly true for the compound **1**, in which the overlap S_1 is maximum.

In spite of all the synthetic and theoretical limitations mentioned, this work shows that it is possible to tune the S–T gap in μ-oxalato copper(II) complexes between zero and −385.4 cm^{-1}. This result is achieved by using some quite simple concepts and by choosing the nature of the terminal ligands. The synthesis of dissymmetrical complexes $[LCu(C_2O_4)CuL']^{2+}$ utilizing $LCu(C_2O_4)$ as a ligand largely increases the possibilities in this field.

Experimental Section

Syntheses. [tmen(H_2O)Cu(C_2O_4)Cu(H_2O)tmen](ClO_4)$_2$·1.25H_2O (1). A 741-mg sample (2 × 10^{-3} mol) of copper(II) perchlorate was dissolved in 10 mL of water. A solution of 232 mg (2 × 10^{-3} mol) of tmen in 5 mL of water was added. A clear blue precipitate appeared, which dissolved upon addition of a solution of 102 mg (10^{-3} mol) of lithium oxalate in 10 mL of water. The dark blue solution was then filtered, and single crystals were obtained by slow evaporation. Under vacuum, the compound loses water. Anal. Calcd for $C_{14}H_{38.5}N_4O_{15.25}Cl_2Cu_2$: C, 26.02; H, 4.95; N, 8.66; Cl, 10.97; Cu, 19.67. Found: C, 25.93; H, 5.03; N, 8.63; Cl, 10.98; Cu, 19.23.

1 can be also prepared from tmenCu(C_2O_4)·4H_2O, which was synthesized by following a procedure similar to that for dmenCu(C_2O_4)·H_2O (dmen = *N,N'*-dimethylethylenediamine).[21] A 268-mg sample (10^{-3} mol) of tmenCu(C_2O_4)·4H_2O was dissolved in 20 mL of water. A solution of 370 mg (10^{-3} mol) of copper(II) perchlorate and 116 mg (10^{-3} mol) of tmen in 5 mL of water was then added. The mixture was filtered. Single crystals were obtained by slow evaporation.

[dienCu(C_2O_4)Cu(H_2O)$_2$tmen](ClO_4)$_2$ (2). A 268-mg sample (10^{-3} mol) of tmen Cu(C_2O_4)·4H_2O was dissolved in 20 mL of methanol. A solution of 370 mg (10^{-3} mol) of copper(II) perchlorate and 103 mg (10^{-3} mol) of dien in 10 mL of methanol was then added. A violet blue precipitate of **2** immediately appeared. Single crystals were obtained by slow evaporation from an aqueous solution. Anal. Calcd for $C_{12}H_{33}N_4O_{14}Cl_2Cu_2$: C, 21.57; H, 4.79; N, 10.48; Cl, 10.61; Cu, 19.02. Found: C, 21.76; H, 4.82; N, 10.89; Cl, 10.48; Cu, 19.68.

[tmen(2-MeIm)Cu(C_2O_4)Cu(2-MeIm)tmen](PF_6)$_2$ (3). A solution of 136 mg (2 × 10^{-3} mol) of 2-MeIm in 10 mL of water was added to a solution of 483 mg (2 × 10^{-3} mol) of copper(II) nitrate in 10 mL of water. A clear blue precipitate appeared, which dissolved upon addition of 232 mg (2 × 10^{-3} mol) of tmen. A solution of 134 mg (10^{-3} mol) of sodium oxalate in 5 mL of water and a solution of 326 mg (2 × 10^{-3} mol) of ammonium hexafluorophosphate in 5 mL of water were successively added. **3** partially precipitated in the form of a dark blue powder. Single crystals were obtained by slow evaporation of the remaining solution. The crystals appear in two shapes, rectangular plates and rhombohedra that actually correspond to the same compound. Anal. Calcd for $C_{22}H_{44}N_8O_4F_{12}P_2Cu_2$: C, 29.31; H, 4.88; N, 12.43; P, 6.88; Cu, 14.10. Found: C, 29.38; H, 4.78; N, 12.41; P, 7.09; Cu, 14.47.

Table VI. Crystallographic Data

	1	2	3
cryst syst	triclinic	monoclinic	triclinic
space group	$P\bar{1}$	$P2_1/c$	$P\bar{1}$
a, Å	18.955 (5)	11.821 (4)	8.224 (3)
b, Å	10.019 (3)	9.093 (3)	10.414 (3)
c, Å	7.658 (3)	23.998 (6)	11.754 (3)
α, deg	98.30 (3)	90	94.63 (2)
β, deg	98.37 (3)	96.50 (4)	108.57 (2)
γ, deg	88.19 (2)	90	103.15 (2)
V, Å^3	1424	2563	916
mol wt	704.97	668.40	901.66
Z	2	4	1
ρ_x, g cm^{-3}	1.64	1.73	1.63

Table VII. Data Collection for Compounds **1** and **3**

General Conditions
temp: 293 K
radiation: molybdenum, λ(Kα) = 0.710 69 Å
monochromatization: oriented graphite crystal
crystal-detector dist: 207 mm

Specific Conditions for **1**
takeoff angle: 6°
scan mode: θ-θ
max Bragg angle: 28° (s = 0.661)
scan angle: $\Delta\theta = [\Delta\theta_0{}^a + B^a \tan\theta]°$; $\Delta\theta_0$ = 1.20°, B = 0.35
detector window: height = 4 mm; width = [2.40 + 1.20 tan θ] mm
scan speed: SIGPRE^a = 0.500; SIGMA^a = 0.010; VPRE^a = 7° min^{-1}; TMAX^a = 60 s
std reflcns: intensity $\bar{7}30$, $\bar{4}3\bar{2}$, $\bar{2}1\bar{3}$ (checked every 3600 s); orientation 10,0,0, 060, 006 (checked every 100 reflcns)
crystal morphology: spherical polyhedron with $\bar{R}$ = 0.045 cm
abs factor: $\mu_{Mo\ K\alpha}$ = 17.55 cm^{-1}
independent reflcns collected: 6755; 5667 with $I > 3\sigma(I)$
reflcns used in refinement: 3203 with $I > 3\sigma(I)$ and $s < 0.528$

Specific Conditions for **3**
takeoff angle: 2.4°
scan mode: θ-0.33θ
max Bragg angle: θ = 26° (s = 0.617)
scan angle: $\Delta\theta = [0.80 + 0.35 \tan\theta]°$
detector window: height = 4 mm; width = 4 mm
scan speed: SIGPRE^a = 0.500; SIGMA^a = 0.018; VPRE^a = 10° min^{-1}; TMAX^a = 60 s
std reflcns: intensity $3\bar{3}1$, 005, 006, $3\bar{7}\bar{4}$ (checked every 3600 s); orientation $6\bar{9}\bar{4}$, 065, $\bar{3}74$ (checked every 100 reflcns)
crystal morphology: triclinic prism; dimensions 0.050 × 0.064 × 0.010 cm; face indices (001), (00$\bar{1}$), (10$\bar{1}$), ($\bar{1}$01), (010), (0$\bar{1}$0)
abs factor: $\mu_{Mo\ K\alpha}$ = 14.01 cm^{-1}
transmission factor range: 0.525–0.876
independent reflcns collected: 3652
reflcns used in refinement: 3633 with $I > 3\sigma(I)$

[a] These parameters have been defined by: Mosset, A.; Bonnet, J. J.; Galy, J. *Acta Crystallogr., Sect. B* 1977, *B33*, 2633.

Crystallographic Data. Preliminary precession photographs showed triclinic symmetry for **1** and **3** while **2** was found to crystallize as monoclinic with space group $P2_1/c$. Single crystals of **1** and **3** were mounted on an Enraf-Nonius CAD-4 computer-controlled four-circle diffractometer. For **2**, we used a Philips four-circle diffractometer. Accurate unit-cell constants were derived from least-squares refinements of the setting angles of 25 reflections. They are reported in Table VI. Information on the data collections are summarized in Tables VII and VIII.

Structure Refinements. Refinements of the three structures were performed by full-matrix least-squares techniques. Throughout the refinement the function minimized was $\sum w(|F_o| - |F_c|)/\sum|F_o|$, where

(32) Charlot, M. F.; Verdaguer, M.; Journaux, Y.; de Loth, P.; Daudey, J. P. *Inorg. Chem.*, preceding paper in this issue.
(33) Girerd, J. J.; Journaux, Y.; Kahn, O. *Chem. Phys. Lett.* **1981**, *82*, 393–398.

Table VIII. Data Collection for Compound **2**

temp: 293 K
radiation: molybdenum, $\lambda(K_\alpha) = 0.71069$ A
monochromatization: oriented graphite crystal
crystal-detector dist: 207 mm
takeoff angle: 6°
scan mode: ω–2θ
scan speed: 0.05° s^{-1}
max Bragg angle: 20°
scan angle: $\Delta\theta = [0.90 + 0.30 \tan\theta]°$
detector window: height = 3 mm; width = 3 mm
std reflcns: $4\bar{6}4$, 12,2,$\bar{1}$, $\bar{4}6\bar{4}$ (checked every 7200 s)
crystal morphology: parallelepiped prism;
dimensions 0.05 × 0.03 × 0.035 cm
abs factor: $\mu_{Mo\ K\alpha} = 18\ cm^{-1}$
reflcns used in refinement: 2985 with $I > 4\sigma(I)$

Table IX. Positional Parameters for the Atoms of $[tmen(H_2O)Cu(C_2O_4)Cu(H_2O)tmen](ClO_4)_2 \cdot 1.25H_2O$ (1)

atom	x	y	z
Cu(1)	0.08744 (4)[c]	−0.17225 (7)	−0.1365 (1)
Cu(2)	0.41771 (4)	0.32775 (7)	−0.2122 (1)
Cl(1)	0.12379 (9)	0.2382 (2)	0.3820 (2)
Cl(2)	0.3524 (1)	−0.2584 (2)	0.2524 (3)
O(1)p(1)	0.1560 (5)	0.2196 (9)	0.547 (1)
O(2)p(1)	0.1656 (6)	0.1632 (9)	0.272 (2)
O(3)p(1)	0.0567 (4)	0.1867 (8)	0.341 (1)
O(4)p(1)	0.1294 (3)	0.3707 (6)	0.353 (1)
O(1)p(2)	0.2992 (6)	−0.288 (1)	0.340 (1)
O(2)p(2)[a]	0.3719 (9)	−0.379 (2)	0.166 (2)
O(3)p(2)[a]	0.4097 (9)	−0.233 (2)	0.396 (2)
O(4)p(2)[a]	0.342 (1)	−0.149 (2)	0.161 (3)
O(5)p(2)[a]	0.4228 (9)	−0.303 (2)	0.278 (2)
O(6)p(2)[a]	0.3453 (8)	−0.121 (2)	0.232 (2)
O(7)p(2)[a]	0.329 (1)	−0.323 (2)	0.065 (2)
O(1,1)	0.0588 (2)	0.0180 (4)	−0.1486 (5)
O(2,1)	0.0217 (2)	−0.1625 (4)	0.0430 (5)
O(1,2)	0.4800 (2)	0.3361 (4)	0.0203 (5)
O(2,2)	0.4482 (2)	0.5157 (4)	−0.2018 (6)
N(1,1)	0.1343 (3)	−0.1899 (5)	−0.3583 (7)
N(2,1)	0.1082 (3)	−0.3692 (5)	−0.1306 (7)
N(1,2)	0.3990 (3)	0.1297 (5)	−0.2301 (7)
N(2,2)	0.3772 (3)	0.3145 (5)	−0.4716 (6)
C(1)	0.0114 (3)	0.0529 (6)	−0.0559 (8)
C(2)	0.5093 (3)	0.4471 (6)	0.0635 (8)
C(1,1)	0.1492 (4)	−0.3351 (6)	−0.4072 (9)
C(2,1)	0.1658 (4)	−0.4026 (6)	−0.2409 (9)
C(1,2)	0.3438 (4)	0.1011 (7)	−0.3880 (9)
C(2,2)	0.3615 (4)	0.1710 (7)	−0.5348 (9)
C(3,1)	0.2021 (4)	−0.1128 (8)	−0.323 (1)
C(4,1)	0.0886 (4)	−0.1386 (7)	−0.5080 (9)
C(5,1)	0.1325 (4)	−0.4016 (7)	0.0519 (9)
C(6,1)	0.0441 (4)	−0.4478 (7)	−0.2037 (9)
C(3,2)	0.3716 (4)	0.0899 (7)	−0.075 (1)
C(4,2)	0.4656 (4)	0.0538 (8)	−0.255 (1)
C(5,2)	0.3110 (4)	0.3980 (8)	−0.492 (1)
C(6,2)	0.4275 (4)	0.3633 (8)	−0.5770 (9)
OW(1)	0.1824 (3)	−0.0916 (5)	0.0855 (7)
OW(2)	0.3198 (3)	0.3980 (5)	−0.0736 (7)
OW(3)	0.1951 (3)	0.2567 (6)	−0.0709 (8)
OW(4)[b]	0.352 (2)	−0.248 (3)	−0.262 (4)

[a] Occupancy 50%. [b] Occupancy 25%. [c] Estimated standard deviations in the last significant figure in this and subsequent tables are given in parentheses.

$|F_o|$ and $|F_c|$ are the observed and calculated structure factor amplitudes and the weight w is $4F_o^2/|\sigma(F_o^2)|^2$. The reliability coefficients are $R = \sum(|F_o| - |F_c|)/\sum|F_o|$ and $R_w = |\sum w(|F_o| - |F_c|)^2/\sum wF_o^2|^{1/2}$. The atomic scattering factors for all atoms and the anomalous terms for Cu, Cl, and P are taken from ref 34.

(34) Cromer, D. T.; Waber, J. T. "International Tables for X-ray Crystallography"; Kynoch Press: Birmingham, England, 1974; Vol. IV, Table 2.2 A. Cromer, D. T. *Ibid.*, Table 2.3.1.
(35) Galy, J.; Bonnet, J. J.; Anderson, S. *Acta Chem. Scand., Ser. A* **1979**, *A33*, 383–389.
(36) Sletten, J. *Acta Chem. Scand., Ser. A* **1983**, *A37*, 569–578.

Table X. Positional Parameters for the Atoms of $[dienCu(C_2O_4)Cu(H_2O)_2tmen](ClO_4)_2$ (2)

atom	x	y	z
Cu(1)	0.2318 (1)	0.2496 (1)	0.3921 (1)
Cu(2)	0.5289 (1)	0.1613 (1)	0.2403 (1)
OW(1)	0.3858 (13)	0.3805 (17)	0.4623 (6)
OW(2)	0.1042 (13)	0.1141 (14)	0.3054 (6)
O(1)	0.4284 (4)	0.3689 (5)	0.2784 (2)
O(2)	0.4461 (4)	0.0742 (5)	0.2990 (2)
O(3)	0.2939 (5)	0.3783 (5)	0.3379 (2)
O(4)	0.3402 (5)	0.1050 (6)	0.3680 (3)
C(1)	0.3863 (6)	0.1534 (6)	0.3270 (3)
C(2)	0.3691 (6)	0.3156 (8)	0.3124 (3)
N(1)	0.1042 (6)	0.3837 (8)	0.4066 (3)
N(2)	0.6124 (5)	0.2670 (6)	0.1858 (3)
N(3)	0.6762 (6)	0.1611 (8)	0.2883 (3)
N(4)	0.4083 (6)	0.1349 (7)	0.1753 (3)
N(5)	0.1908 (8)	0.1197 (8)	0.4543 (3)
C(3)	0.7354 (8)	0.2410 (10)	0.2015 (4)
C(4)	0.7587 (8)	0.2569 (10)	0.2637 (4)
C(5)	0.0520 (13)	0.3163 (17)	0.4535 (8)
C(9)	0.1656 (10)	−0.0334 (12)	0.4347 (5)
C(8)	0.1429 (11)	0.5381 (12)	0.4205 (6)
C(6)	0.5638 (9)	0.2231 (10)	0.1293 (4)
C(7)	0.4376 (10)	0.2246 (10)	0.1276 (4)
C(10)	0.2880 (20)	0.1114 (20)	0.4981 (7)
C(11)	0.0951 (19)	0.1905 (20)	0.4737 (9)
C(12)	0.0183 (13)	0.3920 (17)	0.3577 (7)
Cl(1)	0.6708 (4)	0.3249 (4)	0.4365 (1)
Cl(2)	0.1065 (2)	0.3244 (4)	0.1729 (2)
O(1)Cl(1)	0.6289 (10)	0.3052 (14)	0.4873 (6)
O(2)Cl(1)	0.5892 (10)	0.3350 (14)	0.3919 (5)
O(3)Cl(1)	0.7483 (16)	0.4729 (25)	0.4349 (8)
O(4)Cl(1)	0.7563 (15)	0.2116 (21)	0.4258 (8)
O(1)Cl(2)	0.0038 (12)	0.2842 (15)	0.1872 (6)
O(2)Cl(2)	0.1008 (15)	0.2572 (21)	0.1207 (8)
O(3)Cl(2)	0.1971 (18)	0.3367 (25)	0.2054 (9)
O(4)Cl(2)	0.1658 (16)	0.1945 (23)	0.2113 (8)
O(5)Cl(2)	0.0948 (29)	0.4885 (41)	0.1525 (14)
O(6)Cl(2)	0.0616 (31)	0.4348 (47)	0.2104 (17)
O(7)Cl(2)	0.1728 (39)	0.3958 (58)	0.1404 (20)

$[tmen(H_2O)Cu(C_2O_4)Cu(H_2O)tmen](ClO_4)_2 \cdot 1.25H_2O$ (1). The centrosymmetric space group $P\bar{1}$ was adopted. The positions of the Cu and Cl atoms were deduced from the Patterson map and refined along with the scale factor. The ensuing Fourier synthesis permitted localization of the atoms of the tmen ligands and of oxalato bridges and the oxygen atoms of the ClO_4^- anions. An isotropic refinement resulted in $R = 0.19$ and $R_w = 0.25$ but gave abnormally high thermal parameters for some oxygen atoms of perchlorate p(2), suggesting a disordered arrangement. The disorder was confirmed and resolved from a difference Fourier synthesis, which moreover revealed the water oxygen atoms OW(1), OW(2), and OW(3). A refinement with anisotropic thermal parameters for Cu, Cl, and O atoms, for N atoms of tmen, and for the C_2O_4 groups and isotropic ones for the other atoms yielded $R = 0.088$ and $R_w = 0.117$. A series of alternating difference Fourier maps and least-squares cycles permitted us to discover the fourth water molecule W(4) with partial occupancy and to find most of the hydrogen atoms (those of water molecules W(3) and W(4) were not visible). The non-hydrogen atoms, except those bonded to Cl(2), were treated as anisotropic scatterers, and the hydrogen atoms were included as fixed contributions with isotropic thermal parameters equal to the equivalent B of atoms to which they are attached. In the last cycle of refinement the highest variable shift/esd ratios were less than 50% for oxygen atoms of the disordered ClO_4^- p(2) and less than 16% for other atoms. The reliability factors stabilized at $R = 0.052$ and $R_w = 0.063$ for 3204 observations with $I > 3\sigma(I)$ and $(\sin\theta)/\lambda < 0.528$ and 330 variables. The error in an observation of unit weight was 2.03 electrons. The final difference Fourier map did not show peaks higher than 1% of peaks corresponding to carbon atoms in the final Fourier map. Refined positional parameters for non-hydrogen atoms are listed in Table IX.

$[dienCu(C_2O_4)Cu(H_2O)_2tmen](ClO_4)_2$ (2). The positions of the metal atoms were deduced from the Patterson map and refined along with the scale factor. A Fourier difference series localized all the other atoms but the hydrogen atoms. The refinement with anisotropic thermal parameters on the non-hydrogen atoms converged to $R =$

Table XI. Positional Parameters for the Atoms of [tmen(2-MeIm)Cu(C_2O_4)Cu(2-MeIm)tmen](PF_6)$_2$ (3)

atom	x	y	z
Cu	0.28421 (3)	0.15979 (3)	0.18537 (2)
P	0.0802 (1)	0.36055 (9)	−0.31064 (8)
F(1)	0.2407 (5)	0.3841 (4)	−0.3553 (4)
F(2)	−0.0734 (6)	0.3375 (4)	−0.2588 (6)
F(3)[a]	0.156 (1)	0.5053 (6)	−0.241 (1)
F(4)[a]	0.006 (2)	0.216 (1)	−0.375 (1)
F(5)[a]	0.217 (2)	0.313 (1)	−0.2101 (8)
F(6)[a]	−0.064 (1)	0.400 (2)	−0.401 (1)
F(7)[b]	0.176 (2)	0.439 (2)	−0.1841 (8)
F(8)[b]	−0.010 (2)	0.296 (2)	−0.450 (1)
F(9)[b]	0.089 (2)	0.227 (2)	−0.274 (3)
F(10)[b]	0.043 (2)	0.489 (1)	−0.357 (1)
O(1)	0.0116 (2)	0.0355 (2)	0.1502 (1)
O(2)	0.2034 (2)	0.1033 (2)	0.0054 (2)
N(1)	0.3444 (3)	0.2221 (3)	0.3653 (2)
N(2)	0.2609 (3)	0.3490 (2)	0.1615 (2)
N(3)	0.4187 (3)	0.0215 (2)	0.2059 (2)
N(4)	0.6193 (4)	−0.0783 (3)	0.1946 (3)
C(1)	−0.0552 (3)	−0.0196 (2)	0.0421 (2)
C(2)	0.2719 (5)	0.3413 (4)	0.3688 (3)
C(3)	0.3241 (5)	0.4289 (3)	0.2842 (3)
C(4)	0.2527 (6)	0.1207 (4)	0.4212 (3)
C(5)	0.5388 (5)	0.2565 (5)	0.4350 (3)
C(6)	0.0749 (4)	0.3472 (3)	0.0928 (3)
C(7)	0.3745 (5)	0.4096 (3)	0.0939 (4)
C(8)	0.5707 (4)	0.0354 (3)	0.1853 (3)
C(9)	0.4921 (6)	−0.1690 (4)	0.2170 (4)
C(10)	0.3669 (4)	−0.1081 (3)	0.2242 (3)
C(11)	0.6713 (6)	0.1557 (4)	0.1573 (6)

[a] Occupancy 59%. [b] Occupancy 41%.

0.078. At this stage, a difference Fourier map revealing most hydrogen atoms was calculated. The refinement of their positional parameters was carried out by using the thermal parameters of the corresponding heavy atoms at the end of the isotropic refinement. The refinement including all atoms and all observed reflections converged to $R = 0.064$ for 2985 reflections with $I > 4\sigma(I)$ and $2\theta < 50°$. Refined positional parameters for non-hydrogen atoms are listed in Table X.

[tmen(2-MeIm)Cu(C_2O_4)Cu(2-MeIm)tmen](PF_6)$_2$ (3). As for **1**, space group $P\bar{1}$ was assumed. The Patterson map was used to locate the copper atom. P, O, and N and then C atoms were localized in two steps of alternating least-squares cycles and Fourier synthesis. A refinement with isotropic thermal parameters gave $R = 0.20$ and $R_w = 0.29$. The not surprising disorder of the PF_6^- anion could be only partly resolved from the ensuing difference Fourier map; the introduction of some fluorine atoms in the next cycle of refinement lowered the reliability factors to $R = 0.15$ and $R_w = 0.20$. They were further improved by assigning the Cu, P, O, and N atoms an anisotropic description of thermal motions ($R = 0.10$, $R_w = 0.15$), and the subsequent difference Fourier map was accurate enough to resolve the disorder of PF_6^- and hence to obtain $R = 0.077$ and $R_w = 0.110$. The positions of H atoms were read on the following difference Fourier map and introduced in the least-squares calculations as fixed scatterers with isotropic B factors set equal to the equivalent ones of atoms to which they are bonded. In the last cycle of refinement the highest variable shift/esd ratios were less than 20% for non-fluorine atoms and about 100% for some fluorine atoms. The reliability factors stabilized at $R = 0.038$ and $R_w = 0.057$ for the 3633 observations with $I > 3\sigma(I)$ and 262 variables. The error in an observation of unit weight was 1.98 electrons. Highest peaks in the final difference Fourier map were about $^1/_{15}$th of peaks corresponding to carbon atoms in the final Fourier map. Refined positional parameters for non-hydrogen atoms are listed in Table XI.

Magnetic Measurements. These were carried out with a Faraday type magnetometer equipped with a continuous-flow cryostat working in the temperature range 1.8-300 K. The polycrystalline powder samples weighed about 7 mg. The independence of the susceptibility with regard to the magnetic field was checked at room temperature. Mercury tetrakis(thiocyanato)cobaltate(II) was used as a susceptibility standard. Diamagnetic corrections were estimated as -300×10^{-6}, -300×10^{-6}, and -460×10^{-6} cm^3 mol^{-1} for **1**, **2**, and **3**, respectively.

Acknowledgment. We are most grateful to E. Philippot and R. Astier of the Université des Sciences et Techniques du Languedoc, Montpellier, for collecting intensities of compound **1**.

Registry No. **1**, 83928-09-0; **2**, 83928-11-4; **3**, 92220-60-5; tmenCu(C_2O_4)·4H_2O, 35821-85-3.

Supplementary Material Available: Listings of structure factor amplitudes for compounds **1-3** (53 pages). Ordering information is given on any current masthead page.

Contribution from the Department of Chemistry, Simon Fraser University, Burnaby, British Columbia, Canada V5A 1S6

Structure of the Transition State for Water Exchange on Hexaaquo Divalent Metal Ions

KENNETH E. NEWMAN* and KIM M. ADAMSON-SHARPE

Received October 28, 1983

From a classical electrostatic potential related to that used by Basolo and Pearson, the minimum-energy transition-state structures for water exchange on Ca^{2+}, Mn^{2+}, and Zn^{2+} have been calculated. The results suggest that, in accord with the volumes of activation obtained by high-pressure nuclear magnetic resonance by Merbach and co-workers, at the transition state, metal ions on the right of the periodic table show considerably more extension of their exchanging ligands than those on the left. The potential was also checked by comparing the calculated energies of small alkali-metal ion–water clusters with those obtained by high-pressure mass spectrometry by Dzidic and Kebarle.

Introduction

The development of the dynamics of inorganic reactions owes much to the pioneering book of Basolo and Pearson[1] originally published in 1958. Particularly important was the demonstration that the bond energies of aquo, chloro, and ammine complexes of typically "hard" metal ions could be well calculated in terms of a simple, "soft" charged sphere–polarizable dipole model. Such ideas date right back to the 1920s and have been used both prior to and since Basolo and Pearson's work, but they were particularly successful in demonstrating the soundness of the method by comparing different ligands, different geometries, and different metal ion charges. More recently, Dzidic and Kebarle[2] have measured directly gas-phase alkali-metal ion–water solvation equilibria as a function of temperature by using high-pressure mass spec-

(1) Basolo, F.; Pearson, R. G. "Mechanisms of Inorganic Reactions"; Wiley: New York, 1967; Chapter 2.

(2) Dzidic, I.; Kebarle, P. *J. Phys. Chem.* **1970**, *74*, 1466-1474.

0020-1669/84/1323-3818$01.50/0